Rods to self-avoiding walks to trees in two dimensions

Carlos J. Camacho and Michael E. Fisher
Institute for Physical Science and Technology, University of Maryland, College Park, Maryland 20742

Joseph P. Straley
Department of Physics and Astronomy, University of Kentucky, Lexington, Kentucky 40506-0055
(Received 24 March 1992)

The mean-square radius of gyration $\langle R_G^2 \rangle$ and a shape parameter $\Sigma = \langle R_{G\min}^2 \rangle / \langle R_{G\max}^2 \rangle$ are studied as a function of the number of bonds, bends, and branches of self-avoiding lattice trees on the square, triangular, and honeycomb lattices. We identify the universality classes, and exhibit the crossover scaling functions that connect them. We find (despite doubts recently raised) that there is a universal crossover from rods to self-avoiding walks, embodied in $\langle R_G^2 \rangle \sim N^2 U(Nw)$, where $w(z)$ is an appropriately chosen nonlinear scaling field reducing to the stiffness fugacity z as $z \to 0$; that "rigid trees" (which are bond clusters that branch but do not bend) are in the same universality class as branched polymers or free trees; that the crossover from rods to rigid trees has the universal form $\langle R_G^2 \rangle \sim N^2 W(Ny^2)$, where y the branching fugacity; and that the crossover from self-avoiding walks to branched polymers has the universal form $\langle R_G^2 \rangle \sim N^{2\nu_s} Y(Ny^{\phi})$, with $\nu_s = \frac{3}{4}$ and $\phi = \frac{55}{32}$.

PACS number(s): 05.50.+q, 36.20.Ey, 64.60.Ak, 05.70.Fh

I. INTRODUCTION

The work reported here originates in an ongoing [1–5] study of "planar vesicles"—that is, closed self-avoiding chains or polygons embedded in the two-dimensional plane which are, additionally, (a) subject to a pressure differential $\Delta p = p_{\rm int} - p_{\rm ext}$ between interior and exterior and (b) endowed with a rigidity modulus κ which tends to keep successive links of the chain aligned parallel. As the pressure Δp, rigidity κ, and chemical length (measured by N, the number of self-avoiding "beads" or disks) are changed, the sizes and shapes of the vesicles vary markedly. Indeed, they exhibit a number of relatively sharp crossovers and transitions from one form to another [1–5]. In particular, for $\Delta p \simeq 0$ one observes [1,4] flaccid self-avoiding (s) polygons of linear dimensions increasing as N^{ν_s} with $\nu_s = \frac{3}{4}$, while when κ increases, these approach rigid circular shapes of dimensions proportional to N.

If, on the other hand, κ is small and a large *negative* pressure differential is imposed, the flaccid polygons collapse into branched-polymer or *treelike* (t) configurations [1–3] of linear dimensions increasing as N^{ν_t} with $\nu_t \simeq 0.64$. Note that since the interior of a vesicle is minimal in the limit $\Delta p \to -\infty$, each branch of a tree or branched-polymer vesicular configuration has a double-stranded character. When the rigidity κ increases at fixed N, one observes [1,5] initially a reduction in the number of branches. This eventually leads to an unbranched semiflexible chain, which for large N must behave as an open *self-avoiding walk* (SAW; also denoted s) or chain. Then, under further increase of κ, such chains cross over to increasingly straight and rigid *rods* (r) of dimensions proportional to N (or, equivalently, having $\nu_r \equiv 1$).

Recent Monte Carlo simulations [5] of the highly collapsed or deflated regime of vesicles exhibit a rather rapid crossover from the rod to tree forms, associated, indeed, with a relatively sharp specific-heat (or energy-fluctuation) peak. Furthermore, this peak appears to sharpen as $|\Delta p|$ and N increase, suggesting some sort of asymptotically sharp transition. Owing to the double-stranded nature of the vesicular trees, SAW's, and rods, however, the Monte Carlo simulations are hard to bring to equilibrium in this regime. More crucially, theoretical considerations make it difficult to envisage *how* a truly sharp transition might arise in this regime of the model, notwithstanding the suggestive "experimental" data.

For these reasons it is desirable to understand the rigidity-induced crossover from trees to SAW's to rods without the complexity of double strandedness and a direct connection to vesicles. The literature devoted to self-avoiding walks is, of course, very extensive, and trees or branched polymers have also been much studied. However, the effects of rigidity and of a naturally related branching fugacity on the sizes and shapes of trees seem to have attracted rather little attention. In particular, the various crossover regimes and associated *scaling functions* do not seem to have been analyzed; but, to understand the tree-SAW-rod behavior seen in the study of planar vesicles, it is just these crossovers and scaling functions that are needed. The crossover from rigid rods to SAW's has been of interest since early theoretical work on polymers [6]. However, some issues have only recently been broached, and certain puzzles regarding universality have been raised [7].

Accordingly, we have undertaken a primarily numerical study of trees or branched polymers embedded in the two-dimensional plane with a view to understanding their shapes and sizes and associated transformations in these induced by the introduction of rigidity and variable branching. We have chosen to focus on self-avoiding *lat-*

tice trees, utilizing the square, triangular, and honeycomb lattices with the specific intention of identifying and checking universal features in two dimensions. For these lattices we have collected and analyzed shape statistics for trees with regard to topology, specifically the number of *ends* and of the number of *bends* in the graphical embedding of the tree in the lattice. Where data were not available in the literature (or not suitably classified), we have generated and crosschecked further extensive data sets [8].

Our specific classification of graphs is set out in Sec. II, where we introduce fugacities y (for ends) and z (for bends). Both of these fugacities are needed to account for the main effects of the rigidity modulus in highly deflated vesicles: Note, indeed, that the energy scale associated with an "atomically" sharp, "hairpin" bend at the ends of a vesicle collapsed into one double-sided rod should be regarded as being physically distinct from the rigidity energies associated with relatively smooth bending along the length of a flexible rod. Beyond that, of course, it is of independent interest to distinguish both ends and bends. The two-variable space thus defined by y and z contains several special limits: rods (r), self-avoiding walks (s), trees or branched polymers (t), rigid trees with unbent branches (rt), maximally branched trees, and maximally bent trees, as indicated in Fig. 1. In Sec. III we consider the crossover regimes that connect some of these limits: self-avoiding walks to trees, rods to rigid trees, and rods to self-avoiding walks. We discuss whether rigid trees represent a universality class that is distinct from unrestricted trees, concluding that they do not. We also report less detailed explorations of other regions of the phase diagram.

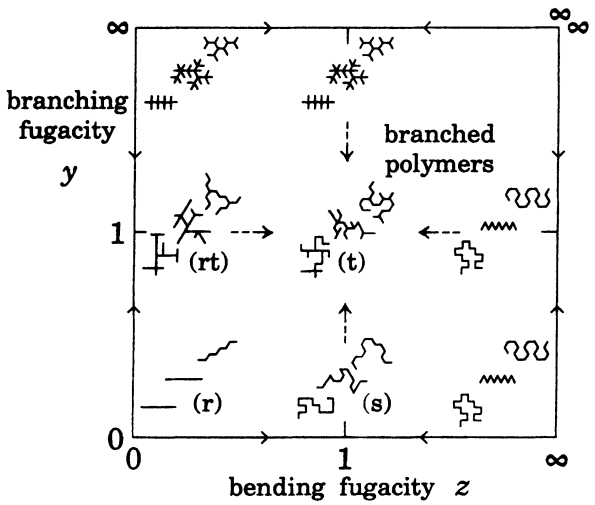

FIG. 1. The (y,z) plane, illustrating the special limiting cases, including rods (r), SAW's (s), trees or branched polymers (t), and rigid trees (rt). The arrow pattern indicates the dominance of the underlying renormalization-group fixed points; more concretely, the arrows point towards the critical models that determine the asymptotic behavior in the intermediate regimes. Typical configurations are presented for the square, triangular, and honeycomb lattices in the limits that y and z are small, large, or of order unity, in all combinations. Note that for $y \to \infty$, the maximally branched trees have a linear structure on the square lattice, but can branch (but not bend) on the triangular and honeycomb lattices, whereas for $z \to \infty$, the maximally bent walks assume linear forms on the triangular and honeycomb lattices, but can bend (but not branch) on the square lattice.

II. CLASSIFYING TREES BY VERTEX TYPE

We idealize branched polymers as self-avoiding loopless graphs or trees on a regular space lattice. Our goal is to determine the critical exponents that characterize their asymptotic behavior, to identify the various universality classes that arise, and to estimate the crossover scaling functions that connect them.

A tree can be classified by the number N of its bonds and by the numbers N_k of its vertices that are shared by k bonds—thus, N_1 is the number of free ends, so that a linear chain polymer has $N_1=2$, $N_2=N-1$, and all other $N_k=0$. There are two constraints on the N_k: For any tree graph one has

$$\sum_{k=1} N_k = N+1 \ , \tag{1}$$

and since every bond joins two sites,

$$\sum_{k=1} kN_k = 2N \ . \tag{2}$$

We further classify a tree by the number of bends B in the linear segments of the tree, defined as follows: On the *square lattice,* a bend is defined to be a site where two (and only two) bonds join at a right angle. There will necessarily be bonds at right angles at any branch site, the number of which is controlled by the number of ends; in our definition we count only the topologically unnecessary bends. Assuming rotational invariance of the weights, the 16 possible assignments of bonds at a vertex can be classified into six distinct types (including the isolated site, which cannot occur as part of a tree); it is sufficient to classify trees by the number of ends N_1, bends B, threefold sites N_3, and bonds N to completely specify the number of sites of each type, because the two graph identities (1) and (2) then fix the number of unbent linear segments as

$$N_{\text{unbent}} = N_2 - B = N + 2 - \tfrac{3}{2}N_1 - \tfrac{1}{2}N_3 - B \tag{3}$$

and fourfold sites as

$$N_4 = \tfrac{1}{2}N_1 - \tfrac{1}{2}N_3 \ . \tag{4}$$

On the *triangular lattice,* there is a richer set of site types, and retaining complete information is impractical. Sites at which exactly two bonds join were classified according to the interior angle formed (60°, 120°, or 180°). At sites where $k=3$, 4, 5, or 6 bonds meet, bends were not distinguished. (The associated bending energies would play a role in distinguishing the different vertex types. Introduction of the corresponding vertex fugacities would make the parameter space much larger and subdivide the data set into an unwieldy number of categories.)

On the *honeycomb lattice,* a bend is defined as a sequence of three bonds in a chain which are in the *cis* conformation. (The bond centers of a honeycomb lattice form the vertices of a kagomé lattice; in terms of this latter structure, we are considering neighbor-avoiding walks, and the bends are defined as on the triangular lat-

tice.) Bends are again not counted at threefold-coordinated vertices, because there is only one type of trivalent vertex, the number of which in a tree is fixed by the number of ends. Thus, in effect these energies have been absorbed into the end fugacities.

The statistical weight of a graph is allowed to depend on the number of bonds, bends, and the population of vertex types; specifically, we define the grand partition function for trees by

$$Q(x,y_k,z)=\sum x^N z^B \prod_k y_k^{N_k} = \sum_{N,B,N_k} C(N,B,N_k) x^N z^B \prod_k y_k^{N_k} , \quad (5)$$

where the first sum is over all graphs that can be embedded per site in the chosen lattice with no overlaps of bonds or vertices; in the second sum, we have introduced the number $C(N,B,N_k)$ of such embeddings per site. The weights x, y_k, and z are fugacities for bonds, vertex type, and bends. Without loss of generality, we may take $y_2=1$. Furthermore, in the studies to be presented here, we have also taken $y_k=1$ for $k>2$. For notational simplicity in what follows, we put $y_1=y$. It is clear that y controls N_1 and thus the degree of branching; however, large z will suppress branching for $y_{k>2}=1$ (see below).

We have counted the graphs on various two-dimensional lattices using the Martin algorithm [9] and for each graph have determined the eigenvalues $\lambda_{\min}\equiv R^2_{G\,\min}$ and $\lambda_{\max}\equiv R^2_{G\,\max}$ of the moment-of-inertia tensor (where each site of the tree is given unit mass). From these we can determine the ensemble average of the radius of gyration, namely,

$$\langle R^2_G(N)\rangle = \frac{\sum_{B,N_1} R(N,B,N_1) z^B y^{N_1}}{\sum_{B,N_1} C(N,B,N_1) z^B y^{N_1}} , \quad (6)$$

and the ensemble average of the absolute difference between the eigenvalues,

$$\langle D(N)\rangle \equiv \langle R^2_{G\,\max}\rangle - \langle R^2_{G\,\min}\rangle = \frac{\sum_{B,N_1} D(N,B,N_1) z^B y^{N_1}}{\sum_{B,N_1} C(N,B,N_1) z^B y^{N_1}} . \quad (7)$$

In fact, we have calculated the coefficients $R(N,B,N_1)$ and $D(N,B,N_1)$ for all $N\le 15$ on the square lattice (and these were further subclassified according to the full set of the N_k), $N\le 11$ on the triangular lattice, and $N\le 18$ on the honeycomb lattice [8]. For certain special cases, longer series were obtained, as noted below. These data are consistent with the previously published series of Gaunt *et al.* [10] and Privman and Redner [11(b)].

The general model contains several others as particular limits; see Fig. 1, which depicts the (y,z) plane. For $y\to 0$, the number of free ends is reduced to $N_1=2$, resulting in the restriction to self-avoiding random walks (for $z\to 1$) and rigid rods (for $z\to 0$). The limit $z=1$, $y=1$ is the ensemble of unrestricted self-avoiding trees, which for consistency with previous work [10,12–15] we may refer to as branched polymers.

For $y=1$, $z\to 0$ the remaining graphs are "rigid trees," which can branch but not bend. This class of graphical embeddings seems not to have been considered previously. Although such rigid trees look somewhat different from branched polymers, one might reasonably guess that they are in the same universality class; we shall give evidence that this is correct. The limit $y\to\infty$ gives "maximally branched trees" for which every site is either an end or a multivalent vertex; on the square lattice, the only such graphs are *combs*, i.e., simply straight rods decorated by the attachment of as many bonds as possible, but on the triangular and honeycomb lattices, the backbone is a neighbor-avoiding branched polymer with no bends (see Fig. 1).

In the limit $z\to\infty$, there are "maximally bent" trees, which on the square lattice are in fact a subclass of the self-avoiding walks, because bending can only occur at two-valent segments, and then maximizing the number of these must decrease the number of multivalent sites. This behavior is something of an artificiality since by setting $y_k=1$ for all $k\ge 3$, the "bending energy" that might naturally be associated with the branching points has been entirely discounted: An alternative two-variable subspace of the full models which will not exhibit this somewhat anomalous behavior could be obtained, e.g., by setting $y_k=1+z^{k-1}$. On the triangular and honeycomb lattices, the maximally bent walks are rigid, linear periodic structures, with no entropy (see Fig. 1).

III. ASYMPTOTIC SCALING BEHAVIOR

For any bounded y and z, the average cluster size grows with x and diverges at some $x_c(y,z)$. Associated with this critical point are the exponents γ and ν defined via

$$Q(x,y,z)\sim (x_c-x)^{-\gamma} , \quad (8)$$

$$\langle R^2_G(N)\rangle \sim N^{2\nu} , \quad (9)$$

which are expected to take universal lattice-independent values characteristic of the different cases illustrated in Fig. 1. In addition, $\langle D(N)\rangle$ is expected to have the same characteristic exponent as $\langle R^2_G(N)\rangle$ but a different amplitude; thus the ratio

$$\Sigma(y,z;N)=\frac{\langle R^2_{G\,\min}\rangle}{\langle R^2_{G\,\max}\rangle}=\frac{\langle R^2_G(N)\rangle-\langle D(N)\rangle}{\langle R^2_G(N)\rangle+\langle D(N)\rangle} \quad (10)$$

should, as $N\to\infty$, approach a quantity characterizing the shape of large clusters. Depending on the values of y and z, the limiting functions $\Sigma(y,z)$ should also display universal aspects [2,3]. The exponents γ and ν can be easily determined for rigid rods, and they are exactly known for self-avoiding walks [16]. Branched polymers are believed [13] to belong to the lattice-animal universality class, which has been extensively studied [14]. These exponents, as well as those that we have estimated for rigid trees and maximally branched trees, are collected in Table I.

TABLE I. Estimates and known values of exponents and critical fugacities for universality classes.

	x_c	γ	ν
Rods	1	1	1
SAW[a]		$\frac{43}{32}$	$\frac{3}{4}$
Branched polymers		0	0.640 ± 0.005
Square	$0.194\,45\pm1$		
Triangular	$0.118_9\pm1$		
Honeycomb	$0.298_3\pm1$		
Rigid trees		0.0 ± 0.05	$0.63_5\pm0.02$
Square	0.2618 ± 4	0.01 ± 0.05	$0.63_5\pm0.02$
Triangular	0.180 ± 7	$0.3_5\pm0.4$	$0.62_5\pm0.02$
Honeycomb	$0.329_5\pm2$	0.05 ± 0.10	$0.63_5\pm0.01_5$

[a]Values of x_c for SAW's are much studied. For some recent estimates for the triangular and square lattices, see Ref. [10(e)]. For the honeycomb lattice, the exact result is believed to be $x_c=1/(2+\sqrt{2})^{1/2}$. See Ref. [16] where the exponent values also are derived.

The critical behavior of Q, Σ, and $\langle R_G^2(N)\rangle$ at intermediate values of y and z combines several of the critical regimes. Our work strongly suggests that the asymptotic behavior, sufficiently close to criticality, is determined by the branched-polymer exponents whenever $0<y<\infty$, $0\le z<\infty$, so that for large N all trees resemble branched polymers in their shape and fractal dimension. This dominance at fixed y and z is indicated by the arrows on Fig. 1. The approach to this limit and the form of the critical surface $x_c(y,z)$ is described by crossover scaling functions. We shall analyze several special cases.

A. Crossover of self-avoiding walks to trees

For $z=1$ and small y, we expect on very general grounds the critical behavior to obey the crossover scaling forms [2,3]

$$Q(x,y,z=1)\approx Ct^{-\gamma_s}Z(Ayt^{-\phi_s}),$$
$$Z(0)=1,\quad Z'(0)=1, \tag{11}$$

$$\langle R_G^2(y,z=1,N)\rangle\approx R_0^2N^{2\nu_s}Y(ByN^{\phi_s}),$$
$$Y(0)=1,\quad Y'(0)=-1, \tag{12}$$

and, for the shape parameter,

$$\Sigma=S(ByN^{\phi_s}), \tag{13}$$

where

$$t=(x_c-x)/x_c \tag{14}$$

is the critical variable for $y=0$. The exponents γ_s and ν_s pertain to SAW's; in two dimensions they take [16] the values $\gamma_s=\frac{43}{32}$ and $\nu_s=\frac{3}{4}$, while ϕ_s is a universal exponent characterizing the crossover from SAW's to branched polymers. The amplitudes A, B, C, and R_0 are nonuniversal metrical constants that can be determined by the normalizations specified in (11) and (12). The amplitude B was chosen by setting the boundary value $Y'(0)=-1$ on the crossover scaling function, implying

$$B=-\frac{C(N,3)}{C(N,2)}\frac{\langle R_G^2(3)\rangle-\langle R_G^2(2)\rangle}{R_0^2N^{2\nu_s+\phi_s}}, \tag{15}$$

where

$$\langle R_G^2(N_1)\rangle=R(N,N_1)/C(N,N_1) \tag{16}$$

and $C(N,N_1)$ is now the number of graphs having N bonds and N_1 ends, while $R(N,N_1)$ is the sum of the squares of the radii of gyration of these graphs.

The scaling functions, normalized as indicated, are expected to be universal. That for the partition function, namely, $Z(u)$, will be singular at some u_c, and near this singularity,

$$Z(u)\approx\frac{Z_c}{(1-u/u_c)^{\gamma_t}}, \tag{17}$$

where γ_t is the branched polymer or tree exponent. In similar fashion, for large arguments $v=ByN^{\phi_s}$, the scaling function for the size must satisfy

$$Y(v)\approx Y_\infty/v^{2(\nu_s-\nu_t)/\phi_s}\quad\text{as } v\to\infty, \tag{18}$$

so that for large N the radius of gyration is always characterized by its tree exponent ν_t. For both large and small arguments the shape scaling function $S(v)$ should approach (generally differing) universal values [3].

In testing the appropriateness of the crossover-scaling forms (11)–(18), the first issue is the value of the crossover exponent ϕ_s. Family [15] has previously studied the crossover from SAW's to branched polymers on the square lattice using a rather crude real-space renormalization-group approximation; his calculations yielded $\phi_s\simeq1.1$.

On the other hand, Gaunt *et al.* [10] have studied the closely related problem of the statistics of lattice trees with fixed topologies. In addition to generating numerical data, Gaunt *et al.* established various rigorous theorems which serve to imply $\phi_s\le2$. Unfortunately, they did not recognize the correct scaling form (11). [See Ref. 10(a), p. 232, where an inadequate scaling hypothesis is presented.] Nevertheless, using their data, they concluded, in effect, that $\phi_s\simeq2$.

If one accepts (11), however, the derivative

$$Q_1(x)\equiv\partial[y^{-2}Q(x,y,z=1)]/\partial y|_{y=0}$$

should diverge as $t^{-\gamma_s-\phi_s}$ at x_c; this generating function counts just the set of three-branched trees (or three-stars) with all possible branch lengths. Similarly, the four-branched trees determine the coefficient of y^4 in Q, which should diverge as $t^{-\gamma_s-2\phi_s}$. We have generated the corresponding series for all three lattices, and studied these using a variety of established series-analysis techniques including differential approximants [17]. This had led to the conclusion

$$\phi_s=1.79\pm0.05. \tag{19}$$

One particularly useful form of analysis is to generate a new series whose nth term is the ratio of the number of graphs having three ends and n bonds to the number of

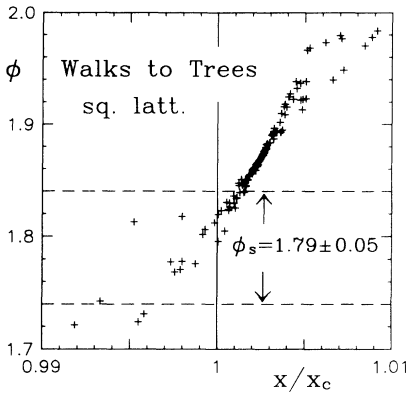

FIG. 2. Estimation of the crossover exponent ϕ_s, from self-avoiding walks to trees (or branched polymers). The + symbols are determined by the singularities of the differential approximants to the generating function $Q_1(x)/Q(x)$ for the square lattice, whose critical point should be at $x/x_c=1$. Similar results are obtained for the triangular and honeycomb lattices.

graphs having two ends and n bonds. This is now a series in x/x_c with a divergence at $x/x_c=1$ characterized by the exponent ϕ_s. The differential approximant analysis of this series is shown in Fig. 2. It is clear from the analysis, however, that rather strong corrections to the leading asymptotic behavior are present.

In striking analytic work, Duplantier [18] has discussed the asymptotic statistics of planar networks of fixed topologies and given general rules yielding the corresponding growth exponents γ. His work implies the result

$$\phi_s=(2d-x_1-x_3)\nu=\tfrac{55}{32}=1.718\,75\ , \tag{20}$$

where the parameters x_k are exponents defined by Duplantier for k-valent network vertices. The difference between this exact result and our estimate (19) is not, we believe, significant, although it is larger than we would wish. It seems likely that our estimate is subject to finite-size ($N\ll\infty$) corrections which, it would seem, converge rather more slowly than our analysis reveals.

To study the validity of the scaling forms for $\langle R_G^2\rangle$ and Σ, we have adopted, first, our estimate (19) and second, the presumably exact value (20). Both values give a reasonable collapse of the data when the limited range of our data is considered. Figure 3 shows the collapse using $\phi_s=\frac{55}{32}$. Figure 4 presents the corresponding analysis for the shape parameter: Note that we have chosen to plot

$$[(N-n_0)/(N+n_0)]^{2\nu_s}\Sigma(y,1;N)$$

rather than $\Sigma(y,1;N)$ itself; here, n_0 is a small offset or "n shift" taking the values $n_0=0.2$ (triangular), 0.15 (square), and 0 (honeycomb) [3,4]. The nonuniversal parameters corresponding to these fits are

$$R_0^2=0.1065\pm0.0005,\quad B=0.0254\pm0.0005\ (\text{sq})\ ,$$
$$R_0^2=0.0989\pm0.0005,\quad B=0.0264\pm0.0010\ (\text{tri})\ ,$$
$$R_0^2=0.1246\pm0.0007,\quad B=0.0229\pm0.0006\ (\text{hc})\ . \tag{21}$$

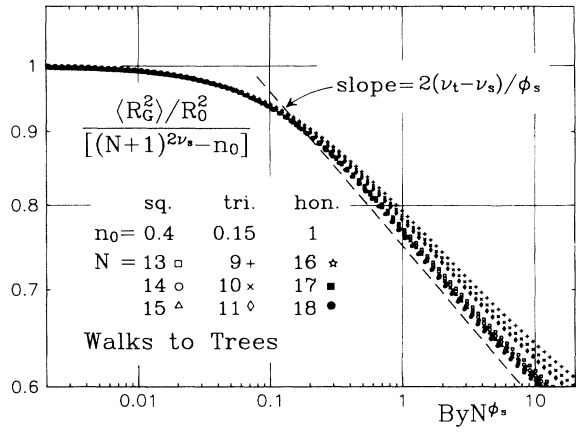

FIG. 3. Estimation of the scaling function for the radius of gyration for crossover from self-avoiding walks to trees (or branched polymers). The plots represent data for the three largest available values of N on the three planar lattices, as a function of the normalized scaled variable ByN^{ϕ_s}, using the theoretical value $\phi_s=\frac{55}{32}$. The plots for other values of N overlap these for small and intermediate y. The dashed line indicates the estimated asymptotic slope for large y, which corresponds to the exponent combination $2(\nu_t-\nu_s)/\phi_s\simeq0.107$. This implies $\nu_t\simeq0.658$, which is reasonably consistent with expectations (see Table I).

At small y, branching is suppressed, and Σ takes on the value 0.15_4, characteristic of SAW's [3]. For large N and $y=1$, there should be a second plateau at a value 0.25_2, characteristic of trees or branched polymers: See Fig. 12, below, and associated discussion. The dashed curve in Fig. 4 for $u\equiv ByN^{\phi_s}>0.6$ indicates the anticipated asymptotic form. However, the data fail to even hint at such behavior! To understand this, note that for the largest trees available, $N=11$ to 18, the scaled variable u

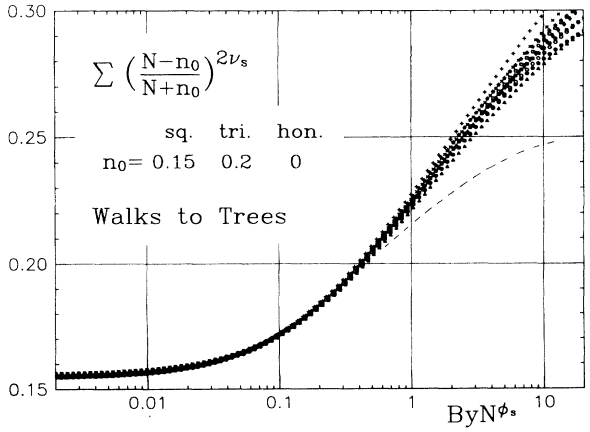

FIG. 4. Crossover scaling function from self-avoiding walks to trees (or branched polymers) for the shape ratio Σ. As in Fig. 3, the plots represent the dependence of the shape factor on the scaled variable yN^{ϕ_s} for the three largest available values of N, with $\phi_s=\frac{55}{32}$. The dashed curve indicates the anticipated asymptotic behavior for large scaled variables (see text).

takes values in the range 1.6 to 3.3 when $y=1$, as appropriate for unconstrained trees. For $u>3$, values of $y>1$ are thus emphasized so that the maximally branched trees (remaining as $y\to\infty$) are weighted increasingly heavily. While we believe that maximally branched trees almost certainly still belong to the universality class of trees, their shapes for finite N are evidently less elongated, and hence they approach asymptotic behavior more slowly.

B. Crossover from rods to rigid trees

For $z=0$ and small y, we study the branching of rigid rods into rigid trees. The crossover scaling functions have the form

$$Q(x,y,z=0)\approx C_r t^{-\gamma_r} X(A_r y t^{-\phi_r}) ,$$
$$X(0)=1, \quad X'(0)=1 \tag{22}$$

$$\langle R_G^2(y,z=0,N)\rangle \approx R_{0r}^2 N^{2\nu_r} W(B_r y N^{\phi_r}) ,$$
$$W(0)=1, \quad W'(0)=-1 \tag{23}$$

and, for the shape parameter,

$$\Sigma = S(B_r y N^{\phi_r}) , \tag{24}$$

but now we have the results

$$\gamma_r=1, \quad \nu_r=1 , \quad \phi_r=2 . \tag{25}$$

These may be demonstrated fairly explicitly by consideration of the expansion of $Q(x,y,z=0)$ in powers of y, in which the coefficient of y^m is the generating function for rigid trees of m branches. For the square lattice one finds this has the form

$$Q(x,y)=2\left[\frac{x}{1-x}\right]y^2+4\left[\frac{x}{1-x}\right]^3 y^3+\left[\frac{x}{1-x}\right]^4 y^4+18\left[\frac{x}{1-x}\right]^5 y^4+12\left[\frac{x}{1-x}\right]^6 y^5+76\left[\frac{x}{1-x}\right]^7 y^5$$
$$+32\left[\frac{x}{1-x}\right]^7\left[1-\left[\frac{1}{1+x}\right]^2\right]y^5+2\left[\frac{x}{1-x}\right]^7 y^6\cdots . \tag{26}$$

Each rigid segment contributes a factor $x/(1-x)$, representing a sequence of bonds of arbitrary length; a tree with k ends contains as many as $2k-3$ rigid segments, if there are no four-valent sites present. Then, each additional end is associated with a factor $y/(1-x)^2$, which corresponds to $\phi_r=2$. A more rigorous argument would have to take into account fully the effects of self-avoidance, which contributes some nonsingular factors (as in the next-to-last term displayed), and of the four-valent sites, which give rise to less singular terms in the expansion (e.g., the third and fifth terms).

Figures 5 and 6 illustrate the collapse of data for the size and shape scaling functions assuming the values (25) for the exponents. Figure 5 also shows a set of curves derived by extrapolation according to the expression displayed: These represent improved estimates of the true, limiting scaling function $W(y)$. Within the limitations of the values of N for which we have data, the same scaling function appears to describe the data for all three lattices with the parameter values

$$R_{0r}^2 = \tfrac{1}{12}\ (\text{tri, sq});\ \tfrac{1}{16}\ (\text{hc}) ;$$
$$B_r \simeq 0.327_2\ (\text{tri});\ 1.160_4\ (\text{sq});\ 0.431_2(\text{hc}) . \tag{27}$$

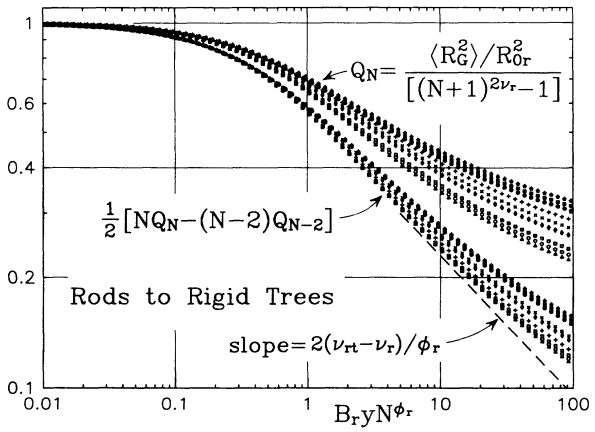

FIG. 5. Crossover scaling plots for rods to rigid trees: the radius of gyration. The symbols have the same significance as in Figs. 3 and 4. Note the extrapolated data sets. The dashed line indicates a power law with exponent $2(\nu_{rt}-\nu_r)/\phi_r \simeq 0.38$, implying $\nu_{rt}\simeq 0.62$ and the expectation, discussed below, $\nu_{rt}=\nu_r\simeq 0.64$.

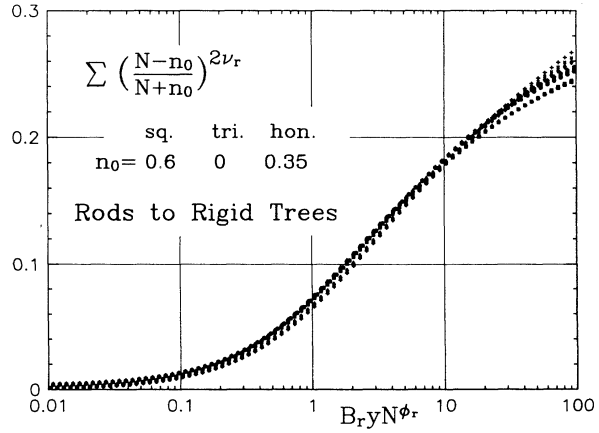

FIG. 6. Crossover scaling plot for rods to rigid trees: shape ratio Σ. The interpretation is the same as for Fig. 4.

C. Crossover from rods to self-avoiding walks

For small z and $y=0$, we might expect the critical behavior to have the general form

$$Q(x,y=0,z)\approx C_r t^{-1} V(Ezt^{-\psi}) ,$$

$$V(0)=1, \quad V'(0)=1 , \tag{28}$$

$$\langle R_G^2(y=0,z,N)\rangle \approx R_{0r}^2 N^{2\nu_r} U(DzN^{\psi}) ,$$

$$\nu_r=1, \quad \psi=1 , \tag{29}$$

where $t=1-z$ is the variable which measures the approach to rigid rod criticality (since $x_c=1$); the appropriate crossover exponent is ψ; and D, E, C_r, and R_{0r} are nonuniversal constants [the last two already appearing in (22) and (23)].

This problem has been considered previously, in particular by Lee and Nakanishi and by Privman and Redner [11]. It appears that $\psi=1$ for all lattices and dimensions $d>1$ (and this applies for closed loops also [11]). However Privman and Redner [11(b)] concluded that the scaling function $U(u)$ is *different* for the square and triangular lattices, so that universal behavior seemed to be limited. Such a breakdown of universality was, indeed, later established analytically by Privman and Frisch [11(c)] for progressive or directed self-avoiding walks. However, the self-avoiding or flexible limit is trivial (in a renormalization-group sense) for such walks, while it is nontrivial for standard self-avoiding walks $1<d<4$. See also Halley *et al.* [11(d)] and Moon and Nakanishi [11(e)] for further discussion of some of these issues.

In our study of this problem we have generated data for random walks on the triangular lattice up to 15 steps, subclassifying the walks according to the number of 60° and 120° turns made, thus allowing for an arbitrary weighting of the two kinds of bends. (Privman and Redner used walks up to length $N=22$ (sq) and 16 (tri), but imposed $z_{60}=z_{120}$.) We have also used a Monte Carlo algorithm (described below) to sample SAW's of 25, 50, and 100 steps on the triangular lattice. (Note also Monte Carlo work for the square lattice by Nakanishi and coworkers [11(a)].)

We find, as did Privman and Redner, that the data for $\langle R_G^2\rangle$ on the different lattices cannot be well represented by a single scaling function of the form of (29) (see Fig. 7). One notes, however, that this representation is not successful in collapsing the data even for a single lattice type once the scaled variable DzN exceeds 10. On the other hand, it must be stressed strongly that for any fixed z in the range, say, 0.3 to 1.3, the SAW-type asymptotic behavior with $\langle R_G^2\rangle \sim N^{3/2}$ is well obeyed even for N as small as 10 to 14 (although the amplitudes necessarily depend on z).

In fact, this dichotomy indicates that the "bare fugacity" z is not the optimal quantity with which to construct the scaled variable to be used as the argument of the scaling function in (29). Rather, as discussed and illustrated in Ref. [4], the fugacity z should be replaced by a *nonlinear scaling field* [19] which we can represent to sufficient accuracy as a function of z only, say, $w(z)$, that behaves like z when $z\to 0$. (Such a nonlinear scaling field has been found to be important also in other contexts [20,21].) Now, in the scaling theory for free random walks with only nearest-neighbor interactions, the rigidity modulus or bending fugacity enters only through its influence on the mean cosine,

$$\langle \cos\theta\rangle = \langle \vec{s}_j\cdot\vec{s}_{j+1}\rangle / a^2 ,$$

between successive steps (with $|\vec{s}_j| \propto a$): See, e.g., Refs. [4, 6, 11(a), 11(e)]. Accordingly, we consider here the corresponding nonlinear variables

$$w(z)=\frac{2z}{1+2z} \quad \text{(square)} \tag{30}$$

$$=\frac{z_{120}+3z_{60}}{1+2z_{60}+2z_{120}} \quad \text{(triangular)} \tag{31}$$

$$=\frac{\frac{1}{2}z}{1+0.6z} \quad \text{(honeycomb)} \tag{32}$$

as candidates for improved scaling fields. For the square and triangular lattices, the choice is just the value of $\langle 1-\cos\theta\rangle$ in terms of z for the corresponding free walk; for the honeycomb lattice, the coefficient 0.6 was chosen empirically as giving the best collapse and match to the other lattice types for low z, although the free random walk would replace 0.6 by $\frac{1}{2}$ (and generate different contributions of order z^3, etc.) [22].

In order to test the proposed forms (30)–(32), the scaled combination in the scaling function in (29) is replaced by $w(z)N^{\psi}$ with $\psi=1$. Figure 8 shows that these assignments for the nonlinear scaling fields are rather successful: Note that the data for the different lattices now agree within good precision for different values of N over the whole range $0\le z\le 1$ [23]. We also found that different choices for weighting bends on the triangular

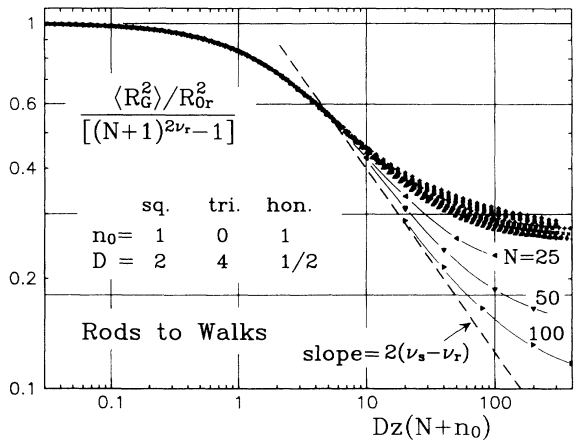

FIG. 7. Crossover scaling plot for $\langle R_G^2\rangle$ for rods to self-avoiding walks. The plots (as constructed from the longest available exact data with $z_{60}=z_{120}=z$) should generate the scaling functions for square, triangular, and honeycomb lattices; also shown are approximate data for the triangular lattice for larger values of N, obtained from Monte Carlo simulations. The data collapse for scaled variable $DzN\ge 10$ is not good. The dashed line indicates the $N^{-1/2}$ behavior required to give $\nu_s=\frac{3}{4}$ for SAW's.

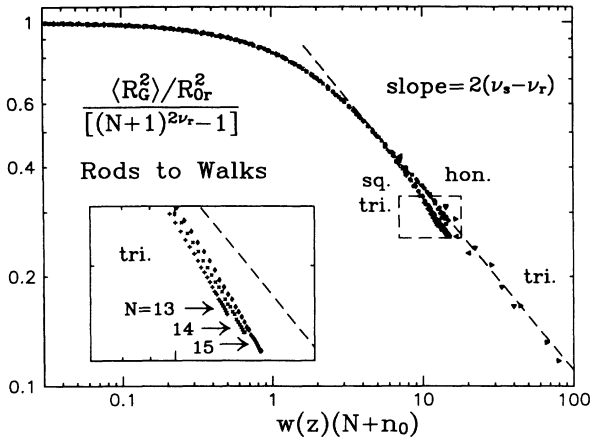

FIG. 8. Crossover function for rods to self-avoiding walks, using the proposed nonlinear scaling variable $w(z)$ in place of z. The main plot superimposes values for the square, triangular, and honeycomb lattices using the same data as in Fig. 7 (although for clarity only one out of every three points has been shown). The Monte Carlo data for the triangular lattice (isolated triangles) for $N=25$, 50, 100 now define fairly precisely an asymptote of expected slope (dashed line), in contrast to Fig. 7. The honeycomb series data for $N=16$–18 appear to have converged quite closely to the same asymptote. The inset shows triangular-lattice data magnified by a factor of 3.7; a distinct trend with increasing N towards the expected asymptote is evident. The square-lattice data behave similarly. Convergence in this region could be improved by adjusting the nonlinear fields slightly.

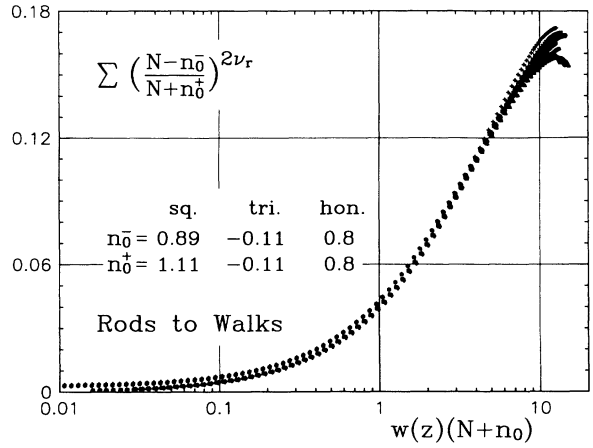

FIG. 9. Crossover scaling plot for the shape ratio $\Sigma(0,z;N)$ for rods to SAW's. The small offsets n_0, with values as in Fig. 7, have been introduced to improve the data collapse for finite N.

lattice (e.g., weighting all bends equally versus giving double weight to 60° bends) led to essentially the same estimate for the scaling function.

Thus we conclude that there is in fact a *universal* scaling description of the size crossover of rods to SAW's [24], although to reveal this for $N \leq 15$, the appropriate nonlinear scaling variable is essential. Note, however, that for $N \gg 15$, it would suffice to use simply zN in all cases, since $w(z)/z \to D$, a constant, as $z \to 0$.

The appropriateness of the nonlinear variable $w(z)$ is further supported by Fig. 9, which shows the corresponding scaling analysis of the shape ratio, which is well represented by

$$\Sigma(y=0,z;N) \approx \left[\frac{N+n_0^-}{N-n_0^+}\right]^2 S[w(z)(N-n_0)] \ . \quad (33)$$

The expected leveling out of the scaling function for large arguments at the value $\Sigma_s = 0.15_4$ is evidently suggested by the plot although the available data are not well converged in this region.

We have also studied the higher moments of the mass distribution functions, and find that these too can be put into universal scaling form using the nonlinear scaling variables defined by (30)–(32); indeed, plots for $\langle R_G^4 \rangle$ and $\langle R_G^6 \rangle$ analogous to Fig. 8 display precisely similar data collapse and trends with increasing N [24].

The Monte Carlo algorithm used to generate long SAW's proceeds as follows. A SAW is represented by the sequence of displacements (along lattice vectors) that takes the walker from site to site. A proposed new SAW is constructed by changing one of these displacements (choosing both the element to be changed and its new value with the aid of a random number generator); this alters the identities of all sites beyond the change. If the proposed SAW is self-avoiding, it is accepted as the new SAW with a probability that depends on the number of bends in the two walks according to the usual Metropolis [25] algorithm. If the proposed SAW fails either of these tests, the old SAW becomes the new one. We found that for $y=1$ the acceptance ratio is slightly greater than 50%. In this way we sampled walks of 25, 50, and 100 steps on the triangular lattice, for the cases $z=0.05$, 0.1, 0.2, 0.5, and 1.

D. Rigid trees and branched polymers

A leading question to be resolved is whether bending is a relevant variable for branched polymers or free trees—that is, whether rigid trees belong to a different universality class than do branched polymers. Differential approximant analysis of the series generated by the rigid trees [i.e., the series expansion of $Q(x,y=1,z=0)$ as defined in (5)] gives very similar exponents, namely, $-0.03 < \gamma_{rt} < 0.08$ against $\gamma_t = 0$ and $\nu_{rt} \simeq 0.63$ against $\nu_t \simeq 0.64$ (see Fig. 10 and Table I).

As a further test, a second set of series were generated, the coefficients of which are the number of trees of N bonds with *exactly one bend;* this is the series representation of $[\partial Q(x,y=1,z)/\partial z]_{z=0}$. These series should diverge at $x_c(y=1,z=0)$ with the exponent $\gamma_{rt}+\psi_{rt}$, where ψ_{rt} is the exponent governing the crossover from rigid trees to branched polymers via the combination $zN^{\psi_{rt}}$. If the two cluster types belong to the same universality class, but with x_c depending on z, the crossover should be trivial and an *effective* crossover exponent $\psi_{rt}=1$ should appear (arising from the shift in x_c). The analysis for the largest available N values for the square lattice is shown in Fig. 11. Taking note of the values of x_c suggested by Fig. 10, the square-lattice data indicate $\gamma_{rt}+\psi_{rt}=0.92\pm0.08$. For the triangular lattice and the

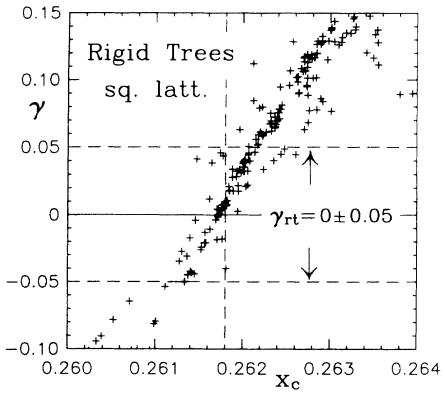

FIG. 10. Differential approximant analysis of the rigid tree series $C(y=1,z=0;N)$ on the square lattice using $N=15$. Each symbol represents one candidate for x_c and γ_{rt}. The accumulation near $x_c=0.2618$ suggests $\gamma_{rt}\simeq 0$.

honeycomb lattice, we estimate $\gamma_{rt}+\psi_{rt}\approx 1.05\pm 0.08$ and 0.90 ± 0.06. These results are somewhat imprecise but are quite consistent with $\psi_{rt}=1$. We conclude that there is most probably *no* singular crossover from rigid trees to free trees or branched polymers.

The estimated shape ratios for rigid trees and branched polymers are also rather similar; Fig. 12 shows the analysis. For both branched polymers and rigid trees (considered independently), the data suggest a universal value $\Sigma=0.25_2\pm 0.01$.

Finally, an intuitive—but quite nonrigorous—argument suggests that $\langle R_G^2(N)\rangle$ must always be larger for rigid trees than for branched polymers: One simply observes that folding something generally makes it smaller. In fact, this is true for the trees we have constructed, as shown in Fig. 13. This would, in turn, imply that ν_{rt} cannot be less than ν_t. Since these exponents are just the asymptotic slopes of the plots in the figure, it also explains why ratio analysis of the series for the two cases tends to suggest a *reversed* exponent inequality: Evidently, the sizes of the rigid trees approach those for free trees or branched polymers from above.

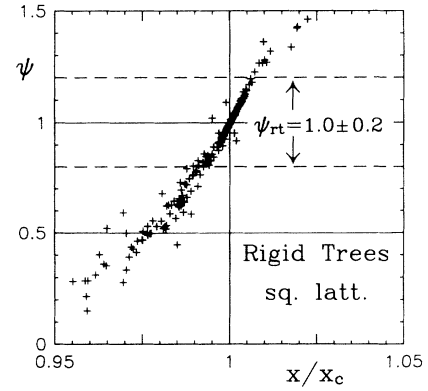

FIG. 11. Analysis of rigid trees with one bend on the square lattice. The plot displays differential approximant estimates for ψ and x_c based on the ratio of $[\partial Q(x,z)/\partial z]_{z=0}$ to $Q(x,0)$.

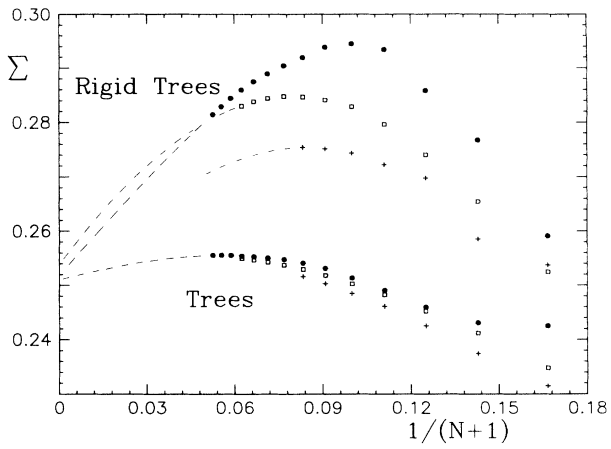

FIG. 12. Shape ratios for branched polymers and rigid trees on the honeycomb (●), square (□), and triangular (+) lattices. The apparent approach of these plots to a value close to $\Sigma=0.25$ suggests they belong to the same universality class. The dashed curves indicate a possible extrapolation to a common limit.

E. Other values of bend and end fugacities

As noted in Fig. 1, even infinite y (maximally branched trees) does not completely suppress bending on the triangular and honeycomb lattices; in fact, the subtrees defined by the interior sites of the lattice configurations represent neighbor-avoiding branched polymers, which can reasonably be expected to lie in the same universality class as branched polymers. Infinite z (maximally bent) trees, on the other hand, do not branch. As noted in Sec. II, this is to a certain extent an artifact of the way we have chosen to define bends. Even then, this serves merely to put these clusters into another of the universality classes that we have already studied—the square lattice gives a variety of SAW's, while on honeycomb and triangular lattices, one obtains rigid rods. As we have seen,

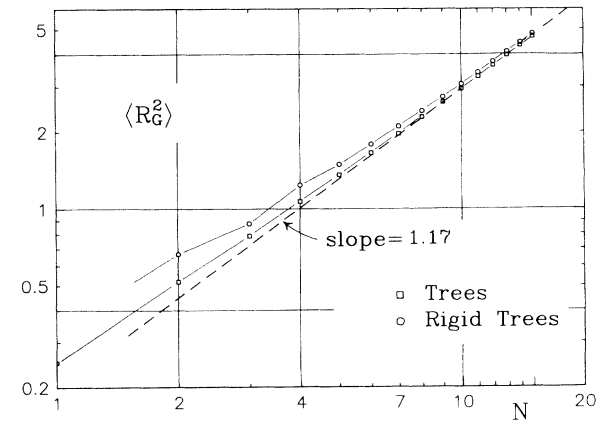

FIG. 13. Logarithmic plot of the radius of gyration $\langle R_G^2(N)\rangle$ for rigid trees and for trees (or branched polymers) on the square lattice. The line of slope 1.17 suggests a possible estimate of $2\nu_{rt}=2\nu_t\simeq 1.17$; however, both plots are still curved for $N=10$ to 15; it is believed that the asymptotic slopes will correspond to $2\nu_{rt}=2\nu_t\simeq 1.28$.

for finite y and z these are unstable relative to branched polymers. Thus, there is no fundamentally new phenomenology exhibited in the phase diagram.

As a check on this for general (finite) values of the fugacities, we have studied the radius of gyration and shape ratio for some other values of y and z. As anticipated, the N dependence of the radius of gyration is well described by

$$\langle R_G^2(y,z,N)\rangle \approx f(y,z)\langle R_G^2(1,1,N)\rangle \ , \tag{34}$$

where for $y,z>0$, $f(y,z)$ is a smoothly varying scale factor. The shape ratio proves somewhat more sensitive to the values of y and z for finite N, but does not contradict the assertion that $\Sigma(y,z;N\to\infty)\simeq 0.25$ for all $0<y$, $z<\infty$, as expected for unrestricted trees or branched polymers.

IV. CONCLUSIONS

In summary, we have studied self-avoiding trees on the triangular, square, and honeycomb lattices subject to a branching fugacity y, which counts monovalent ends, and a bending fugacity z, which counts bends on the tree branches. Of the various special types of configurations appearing, only rods (r: $y=z=0$), self-avoiding walks (SAW's, s: $y=0$, $z>0$), and unrestricted trees or branched polymers (t: $y>0$) appear as distinct universality classes. In particular, rigid trees (rt) seem to belong to the branched-polymer universality class: Both appear to have the same asymptotic value of the shape parameter, namely,

$$\Sigma \equiv \langle R_{G\,\min}^2\rangle / \langle R_{G\,\max}^2\rangle \simeq 0.25_2 \ , \tag{35}$$

whereas self-avoiding walks have $\Sigma\simeq 0.15_4$. (Rods, of course, have $\Sigma=0$.)

We have studied the crossover scaling behavior of the radius of gyration, $\langle R_G^2\rangle$, and the shape ratio, $\Sigma(y,z)$, in various regimes of the phase diagram shown in Fig. 1, specifically: (a) from SAW's to trees [see Eqs. (11)–(14)], where the newly identified crossover exponent $\phi_s=\frac{55}{32}$, which follows from Duplantier's general analysis [18] is confirmed (despite conflicting suggestions in the literature [10]); (b) from rods to rigid trees, where the exact crossover exponent $\phi_r=2$ can be deduced analytically [see Eqs. (22)–(26)]; (c) from rods to SAW's [see Eqs. (28) and (29)], where our exact lattice enumerations have been supplemented by Monte Carlo simulations for $N=25$, 50, and 100. On introducing, via Eqs. (30)–(32), appropriate nonlinear scaling fields [4] embodying the bending fugacity z, the crossover in $\langle R_G^2\rangle$ is observed to be universal over the three lattices (even though this conclusion has been questioned recently [11,24]); (d) rigid trees and unrestricted trees, where an *effective* crossover exponent $\psi_{rt}=1$ corresponds merely to a shift in the critical point $x_c(y,z)$ with, it is concluded, no change in universality class. The various crossover scaling functions for $\langle R_G^2\rangle$ and the shape ratio Σ, of direct relevance to the interpretation of behavior seen in simulations of highly deflating vesicles [1,5] can be read off numerically from Figs. 3–6, 8, and 9. [In these scaling plots the only fitting parameters are small offsets or shifts in the values of N (or N^2) which serve to make some allowances for the leading corrections to asymptotic scaling.]

One outstanding problem not specifically studied here is the determination of the *combined* crossover scaling functions in terms of both the scaled variables yN^2 and zN [or $w(z)N$)] with exponents $\phi_r=2$ and $\psi\equiv\psi_r=1$. This would describe crossover from rods to rigid trees and from rods to SAW's as well as the "direct" crossover from rods to general trees or branched polymers; however, it should also embody, as a special limiting case, the crossover from SAW's to branched polymers as controlled by the Duplantier exponent $\phi_s=\frac{55}{32}$. The data we have amassed [8] would probably suffice for this task, but more sophisticated two-variable methods of analysis (such as partial differential approximants [26]) will probably prove essential for handling the multicriticality entailed.

ACKNOWLEDGMENTS

We are grateful for helpful correspondence with Dr. B. Duplantier, Professor H. Nakanishi, and Professor V. Privman, and assistance from Han Wen. This work has been supported by the National Science Foundation through grants No. DMR 90-03698, No. DMR 90-07811, and No. CHE 86-09722. J.P.S. would like to thank the Institute for Physical Science and Technology of the University of Maryland for their hospitality during his sabbatical visit, when this work was initiated.

[1] S. Leibler, R. R. P. Singh, and M. E. Fisher, Phys. Rev. Lett. **59**, 1989 (1987).

[2] M. E. Fisher, Physica D **38**, 112 (1989).

[3] C. J. Camacho and M. E. Fisher, Phys. Rev. Lett. **65**, 9 (1990).

[4] C. J. Camacho, M. E. Fisher, and R. R. P. Singh, J. Chem. Phys. **94**, 5693 (1991).

[5] C. J. Camacho and M. E. Fisher, in *Computer Simulation Studies in Condensed Matter Physics IV,* edited by D. P. Landau, K. K. Mon, and H. B. Shuttler (Springer-Verlag, Berlin, 1992).

[6] See, e.g., P. J. Flory, *Principles of Polymer Chemistry* (Cornell University, Ithaca, 1953), Chap. X.

[7] See Ref. [4] and references therein.

[8] The resulting data sets have been filed with the AIP document repository. See AIP document No. PAPS PRLAA-46-6300-49 for 49 pages of supplementary data giving the exact lattice counts for honeycomb, square, and triangular lattices classified, as explained in Sec. III, by the number of bonds, ends, bends, and vertices of valence 3 (with some compression for the triangular lattice). A table of Monte Carlo data for $N=15$, 25, 50, and 100 bonds is included

for the triangular lattice for (from 4 to 6) selected values for the bending fugacity. Order by PAPS number and journal reference from American Institute of Physics, Physics Auxiliary Publication Service, 335 East 45th Street, New York, NY 10017. The prepaid price is, currently $1.50 for a microfiche, or $5.00 for a photocopy. Airmail additional.

[9] J. L. Martin, in *Phase Transitions and Critical Phenomena,* edited by C. Domb and M. S. Green (Academic, New York, 1974), Vol. 3, p. 97.

[10] (a) D. S. Gaunt, J. E. G. Lipson, J. L. Martin, M. F. Sykes, G. M. Torrie, S. G. Whittington, and M. K. Wilkinson, J. Phys. A **17**, 211 (1984); for related work see also (b) D. S. Gaunt *et al., ibid.* **17**, 2843 (1984); (c) J. E. G. Lipson *et al., ibid.* **18**, L469 (1985); (d) N. Madras *et al., ibid.* **23**, 5327 (1990); (e) A. J. Guttman and J. Wang, *ibid.*, **24**, 3107 (1991).

[11] (a) S. B. Lee and H. Nakanishi, Phys. Rev. B **33**, 1953 (1986); J. Phys. A **20**, L457 (1987); (b) V. Privman and S. Redner, Z. Phys. B **67**, 129 (1987); (c) V. Privman and H. L. Frisch, J. Chem. Phys. **88**, 469 (1988); (d) J. W. Halley, D. Atkatz, and H. Nakanishi, J. Phys. A **23**, 3297 (1990), and references therein and in (e) J. Moon and H. Nakanishi, Phys. Rev. A **44**, 6427 (1991).

[12] See, for example, (a) T. Ishinabe, J. Phys. A **22**, 4419 (1989), and references therein, including (b) A. J. Guttmann and D. S. Gaunt, *ibid.* **11**, 949 (1978); (c) G. Parisi and N. Sourlas, Phys. Rev. Lett. **46**, 871 (1981); (d) F. Family, J. Phys. A **15**, L583 (1982); (e) D. Dhar, Phys. Rev. Lett. **51**, 853 (1983); (f) Z. V. Djordjevic, S. Havlin, H. E. Stanley, and G. H. Weiss, Phys. Rev. B **30**, 478 (1984).

[13] T. C. Lubensky and J. Isaacson, Phys. Rev. A **20**, 2130 (1979).

[14] See, for example, B. Derrida and D. Stauffer, J. Phys. (Paris) **46**, 1623 (1985); the quoted precision of the estimates may not reflect their true accuracy.

[15] F. Family, J. Phys. A **13**, L325 (1980).

[16] B. Nienhuis, Phys. Rev. Lett. **49**, 1062 (1982).

[17] M. E. Fisher and H. Au-Yang, J. Phys. A **12**, 1677 (1979); **13**, 1517 (1980); D. L. Hunter and G. A. Baker, Jr., Phys. Rev. B **19**, 3808 (1979).

[18] B. Duplantier, Nucl. Phys. B **340**, 491 (1990); see also J. Stat. Phys. **54**, 581 (1989); Phys. Rev. Lett. **57**, 941 (1986).

[19] F. J. Wegner, Phys. Rev. B **5**, 4529 (1972).

[20] D. R. Nelson and M. E. Fisher, Ann. Phys. (NY) **91**, 226 (1975).

[21] A. Aharony and M. E. Fisher, Phys. Rev. Lett. **45**, 679 (1980).

[22] The honeycomb lattice has a two-sublatice structure, so that the usual calculation for continuum random walks or walks on a Bravais lattice does not go through. However, one can develop a matrix analysis which yields the same asymptotic scaling behavior for the crossover of $\langle R_N^2 \rangle$, the mean-square end-to-end distance, but with a more complex expression replacing the mean cosine $\langle \cos\theta \rangle$.

[23] For $z=1$ the limits on the abscissa $u=w(z)(N+n_0)$ are about 6.0, 10.7, and 12 for honeycomb, square, and triangular lattices, respectively. At $u=11$, if no allowance is made for the trend with N seen in the inset in Fig. 8, the approximants for the R_G^2 scaling function for the three lattices agree to within about 6% (or $\pm 3\%$). This deviation would also be reduced by better adjustment of the nonlinear scaling variables $w(z)$. However, Fig. 5 of Ref. [11(b)] indicates a difference of about 5% increasing to 14% in the R_N^2 (or end-to-end) scaling functions for the square and triangular lattices in the range $x \equiv DzN = 4$ to 10. In Fig. 8 here, this corresponds to the range $u \simeq 3$ to 6 where, even without allowance for residual trends with N, the agreement between all three lattices is to within $\pm 1\%$ or less. We believe the larger deviations found in Ref. [11(b)] can probably be attributed to the fact that no allowance was made for the nonlinear scaling fields and similar nonsingular w and N variations.

[24] Note, however, that Privman and Redner [Ref. 11(b)] also studied the crossover in the total number of self-avoiding walks with weighted bends, i.e., the coefficient of x^N in $Q(x,0,z)$, which we have not done. They again found significant differences between the corresponding scaling functions for square and triangular lattices. Note, in fact, that three turns are needed for one self-intersection on the square lattice, while two suffice on the triangular lattice: This is consistent with a difference in scaling functions. It is, indeed, conceivable that these scaling functions are nonuniversal even while those for the size moments and shape ratio are universal, as we find. Further studies would be valuable to elucidate this interesting issue.

[25] N. Metropolis, A. W. Rosenbluth, M. N. Rosenbluth, A. H. Teller, and E. Teller, J. Chem. Phys. **21**, 1087 (1953).

[26] See M. E. Fisher and R. M. Kerr, Phys. Rev. Lett. **39**, 667 (1977); M. E. Fisher and D. F. Styer, Proc. R. Soc. London, Ser. A **384**, 259 (1982); J. H. Chen, M. E. Fisher, and B. G. Nickel, Phys. Rev. Lett. **48**, 630 (1982); and A. J. Guttman, in *Phase Transitions and Critical Phenomena,* edited by C. Domb and J. L. Lebowitz (Academic, London, 1989), Vol. 13, Chap. 1, Sec. 7.